
Robust Counterfactual Explanations for Random Forests

Alexandre Forel

Department of Mathematics and Industrial Engineering
 Polytechnique Montreal
 Montreal, Canada
 alexandre.forel@polymtl.ca

Axel Parmentier

CERMICS
 Ecole des Ponts
 Marne-la-Vallée, France
 axel.parmentier@enpc.fr

Thibaut Vidal

Department of Mathematics and Industrial Engineering
 Polytechnique Montreal
 Montreal, Canada
 thibaut.vidal@polymtl.ca

Abstract

Counterfactual explanations describe how to modify a feature vector in order to flip the outcome of a trained classifier. Several heuristic and optimal methods have been proposed to generate these explanations. However, the robustness of counterfactual explanations when the classifier is re-trained has yet to be studied. Our goal is to obtain counterfactual explanations for random forests that are robust to algorithmic uncertainty. We study the link between the robustness of ensemble models and the robustness of base learners and frame the generation of robust counterfactual explanations as a chance-constrained optimization problem. We develop a practical method with good empirical performance and provide finite-sample and asymptotic guarantees for simple random forests of stumps. We show that existing methods give surprisingly low robustness: the validity of naive counterfactuals is below 50% on most data sets and can fall to 20% on large problem instances with many features. Even with high plausibility, counterfactual explanations often exhibit low robustness to algorithmic uncertainty. In contrast, our method achieves high robustness with only a small increase in the distance from counterfactual explanations to their initial observations. Furthermore, we highlight the connection between the robustness of counterfactual explanations and the predictive importance of features.

1 Introduction

Counterfactual explanations provide a course of action to change the outcome of a classifier and reach a target class. For instance, if a trained classifier rejects the loan application of an individual based on a set of features, a counterfactual explanation method returns the closest feature vector that would lead to the loan being approved. Counterfactual explanations extend traditional machine-learning predictions with a contrastive explanation of “what should be” as opposed to “what is now”. They increase the interpretability of complex machine learning algorithms and provide trust and accountability (Wachter et al., 2017).

The majority of existing methods are based on modifying a given sample until the target class is attained. Thus, they work in a heuristic fashion and do not guarantee that the explanation found is the closest one to the original sample. Optimization approaches based on mixed-integer linear

programming (MILP) can determine counterfactuals that are optimal for the distance metric under consideration and can easily integrate constraints that reflect the actionability of the feature changes (Kanamori et al., 2020). Such methods have proved especially relevant for generating counterfactual explanations over tree ensembles (Cui et al., 2015). Recently, Parmentier and Vidal (2021) have provided a more efficient mixed-integer linear formulation for cost-optimal counterfactuals in tree ensembles.

While many aspects such as actionability and diversity have been discussed, the core issue of counterfactual explanation is to ensure that they are valid. Validity indicates whether the individual can indeed reach a target class by applying the given recourse. In a real context where classification models can be retrained over time, a major challenge is to ensure that the explanations are robust and remain valid after re-training. Interestingly, the issue of algorithmic robustness of counterfactual explanations has not been studied so far. Pawelczyk et al. (2020) studied the transferability of counterfactuals under predictive multiplicity, that is whether a counterfactual explanation derived for a first model is also valid for a second model from a different class (e.g. from a linear regression to a random forest). However, they do not study the more fundamental issue whereby two models from the same class might already output contradicting predictions because of the random training procedure. Likewise, plausibility has been studied extensively and implemented through methods such as density estimation (Artelt and Hammer, 2020), local outlier factor (Kanamori et al., 2020) or local-neighborhood search (Laugel et al., 2019). Plausibility constraints ensure that the counterfactual explanation is not an outlier of the distribution of the target class. However, it remains unclear to what extent plausible counterfactual explanations are robust to algorithmic uncertainty.

The impact of algorithmic uncertainty on the variance of ensemble methods, and especially random forests, has been studied in the past. Most notably, recent works provide insights on the prediction error and on how to identify the forest size with the best trade-off between generalization error and computation time (Probst and Boulesteix, 2017; Lopes, 2019). Our work also relates to the literature on leave-one-out-stability (Bousquet and Elisseeff, 2002), although we focus on the stability of predictions rather than the generalization error of classifiers. Perhaps one of the most closely related streams of research investigates the robustness of counterfactuals to distribution shift: a change in the probability distribution underlying the features and labels. Upadhyay et al. (2021) investigated the robustness of counterfactuals to distribution shift, which they modeled as a change in the classification model parameters. They applied their method to several types of distribution shifts: localization, time, and place. Rawal et al. (2020) studied empirically the distributional robustness of several methods. Finally, Bui et al. (2022) proposed methods based on distributionally robust optimization to improve the robustness of counterfactuals under ambiguous distribution shifts.

Despite the aforementioned contributions, the core problem of algorithmic robustness has not been studied so far in the counterfactual explanations literature. We contribute to the field by proposing new methods to generate counterfactual explanations that are robust to re-training. More specifically, we make the following contributions:

- We derive an efficient formulation to generate robust explanations that uses only the trained random forest and a well-defined threshold. The formulation is based on the link between tree robustness and forest robustness. We also obtain useful properties regarding the robustness of counterfactual explanations in random forests.
- We provide finite-sample and asymptotic robustness guarantees for any random forest using trees with a single decision split (tree stumps) by leveraging existing results in chance-constrained optimization.
- We highlight the fact that naive methods to generate counterfactuals fail to provide robust explanations on common data sets — the validity is often below 50% and falls below 20% on the most complex data set. Furthermore, we show that plausibility is a poor proxy for robustness. Even with very conservative implementations, plausible counterfactual explanations based on isolation forests or the local outlier factor increase the distance of counterfactual explanations but have almost no effect on robustness.
- We demonstrate the performance of our approach on real-world data and measure the trade-off between the distance of counterfactuals and their robustness. We show that our methods provide the Pareto front of dominant solutions on all the data sets considered.
- We study the connection between the predictive importance of features and the robustness of counterfactual explanations. We show that generating robust counterfactuals is especially challenging for data sets with many features with high predictive importance.

2 Problem statement

We consider a binary classification setting with a training sample $Z_n = \{(X_i, Y_i)\}_{i=1}^n$ of size n where $X_i \in \mathcal{X}$ is a vector of features and $Y_i \in \{0, 1\}$ is its associated class. The samples are obtained i.i.d. from an unknown distribution P_{XY} . A (possibly randomized) classification algorithm is applied to the training data to obtain a classifier F^0 with score function $h^0 : \mathcal{X} \rightarrow [0, 1]$. For any new observation $x_{n+1} \in \mathcal{X}$, its predicted class is $F^0(x) = 1$ if $h^0(x_{n+1}) \geq 1/2$ and $F^0(x) = 0$ otherwise. We assume w.l.o.g that the initial class of x_{n+1} is 0, so that the target class of its counterfactual explanation is 1. Given a classifier F^0 trained on Z_n , an optimal counterfactual explanation for x_{n+1} can be found by solving the optimization problem:

$$\min_x f(x, x_{n+1}) \quad (1a)$$

$$\text{s.t. } h^0(x) \geq 1/2 \quad (1b)$$

$$x \in \mathcal{X}^a \cap \mathcal{X}^p. \quad (1c)$$

The objective function in Equation (1a) minimizes the distance between the counterfactual explanation and the original observation. The distance can be expressed as the l_1 or l_2 -norm, or more generally as any feature-weighted distance measure. Constraint (1b) ensures that the class predicted for the counterfactual explanation is the target class. Constraint (1c) specifies that the counterfactual explanation belongs to both the actionable and plausible domains of the feature space. The feasibility constraint specified through domain \mathcal{X}^a ensures that the algorithmic recourse is actionable, i.e. that immutable features are not modified (Ustun et al., 2019). The plausibility domain \mathcal{X}^p ensures that the counterfactual resembles the samples obtained from the data distribution. This is often implemented through constraints that ensure that the counterfactual explanation is not an outlier of the target sample distribution (Kanamori et al., 2020; Parmentier and Vidal, 2021).

Denote the solution of Problem (1) by \hat{x} and let $\mathcal{C}(\cdot; F^0) : \mathcal{X} \rightarrow \mathcal{X}$ be the algorithm that maps any observation x to a counterfactual explanation \hat{x} by solving Problem (1) for the classifier F^0 . Solving Problem (1) provides an actionable counterfactual with minimum distance to its initial observation. The remainder of the paper focuses on extending Problem (1) to generate counterfactual explanations that are robust to algorithmic uncertainty.

2.1 Validity and robustness

In this part, we formalize the concepts of validity and robustness of counterfactual explanations.

Definition 1 (Validity). *Let F^0 and F be two trained classifiers and $\hat{x} = \mathcal{C}(x; F^0)$ be the counterfactual determined for a new observation $x \in \mathcal{X}$ and classifier F^0 . The counterfactual explanation \hat{x} is valid for classifier F if $F(\hat{x}) = F^0(\hat{x})$.*

Definition 2 (Algorithmic robustness). *Let F^0 be a classifier trained on Z_n . A counterfactual algorithm $\mathcal{C}(\cdot; F^0)$ is robust with tolerance α if, for any new observation x_{n+1} , the probability that its counterfactual explanation is valid for a new classifier F trained on Z_n is greater than $(1 - \alpha)$, that is*

$$\forall x_{n+1}, \quad \text{Prob} [F(\mathcal{C}(x_{n+1}; F^0)) = F^0(\mathcal{C}(x_{n+1}; F^0))] \geq 1 - \alpha,$$

where the uncertainty is taken with regards to the random training procedure of F on Z_n .

Notice that a counterfactual algorithm is still robust with tolerance α if its expected validity exceeds $(1 - \alpha)$. Such an algorithm is said to be conservative since it provides a higher validity than required and outputs counterfactuals that are further from their original observations. There is thus a trade-off between the distance of counterfactual explanations as defined in Equation (1a) and their robustness as seen in Definition (2). One of the goals of this work is to investigate the trade-off between these two objectives and to provide robust counterfactuals that remain close to the original observation.

2.2 Random forests

We focus on random forest classifiers (Breiman, 2001) because of their high predictive performance (Biau and Scornet, 2016). A random forest is an ensemble method that averages predictions over many base learners $\{t_i\}_{i=1}^N$. The base learners are decision tree classifiers built for instance following the CART procedure (Breiman et al., 1984). The algorithmic uncertainty of random forests

stems from two factors: (1) each base learner uses a re-sampling of the original training set (most commonly a bootstrap sample or a sub-sample), and (2) a random subset of features is selected at each node of the tree to identify the best split. This randomness improves the prediction accuracy as it reduces the correlation between base learners and significantly reduces variance (see Hastie et al. 2009, Chapter 15, Section 15.4).

For any observation x , denote by $t(x, \xi) \in \{0, 1\}$ the class predicted by a decision tree with random training procedure parameterized by ξ . The score of a random forest using N trees is given by:

$$h_N(x, \xi) = \frac{1}{N} \sum_{i=1}^N t_i(x, \xi_i),$$

where $\xi = \{\xi_i\}_{i=1}^N$ denotes the random training procedure of the forest. The class prediction of a random forest trained on Z_n is thus a random variable. To generate a counterfactual explanation robust to algorithmic uncertainty, Problem (1) is augmented with the probabilistic constraint:

$$\text{Prob}(h_N(x, \xi) \geq 1/2) \geq 1 - \alpha \quad (2)$$

where the probability is taken with regards to the random training procedure of the forest.

3 Robust counterfactual explanations

The core result of our paper is to show that, given a trained random forest F^0 with score function $h_N^0(\cdot, \xi^0)$, we can obtain robust counterfactual explanations by solving the optimization problem:

$$\min_x f(x, x_{n+1}) \quad (3a)$$

$$\text{s.t. } h_N^0(x, \xi^0) \geq \tau \quad (3b)$$

$$x \in \mathcal{X}^a \cap \mathcal{X}^p. \quad (3c)$$

Problem (3) uses only the trees of the initial forest and a well-defined threshold $\tau \in [1/2, 1]$ to ensure algorithmic robustness. Remarkably, Constraint (3b) replaces both the naive Constraint (1b) and the probabilistic Constraint (2). Thus, the computational complexity of the robust problem is the same as the one of the naive problem, and robust counterfactual explanations can be generated easily using existing models such as the one of Parmentier and Vidal (2021).

Deriving Problem (3) comprises two essential steps: (i) reformulating the robustness constraint on forests into an equivalent constraint on trees, and (ii) showing that the probability of any tree to predict the target class is well approximated by the score function of the initial forest. The remainder of this section details these two steps. We also study properties of the tree robustness formulation, and present robustness guarantee for forests made of stumps.

3.1 Reformulating the robustness constraint: from the forest to the tree

For any observation $x \in \mathcal{X}$, the event that a decision tree trained on Z_n outputs the target class at x can be seen as a random event with probability $p(x)$. Thus, the class predicted by a decision tree follows a Bernoulli distribution as $t(x, \xi) \sim \text{Bernoulli}(p(x))$. It follows that the sum of tree predictions of any random forest with N base learners follows a binomial distribution: $N \cdot h_N(x, \xi) \sim \text{Bin}(N, p(x))$. Denote by $B(k; N, p)$ the c.d.f. of the binomial distribution $\text{Bin}(N, p)$ evaluated in k . We start by introducing the following lemma.

Lemma 1. *Given $N \in \mathbb{N}$, the map $g_N : [0, 1] \rightarrow [0, 1], p \mapsto B(N/2; N, p)$ is decreasing and invertible.*

The proof is based on the link between the c.d.f. of the binomial distribution and the c.d.f. of the beta distribution. It is given in Supplementary Material A.1. Using a binomial model for the class predicted by a random forest and Lemma 1, we can now reformulate the robustness constraint on a forest into a robustness constraint on a tree.

Theorem 1. *Let h_N be the random score function of a random forest with N base learners trained on Z_n . The condition $\text{Prob}(h_N(x, \xi) \geq 1/2) \geq 1 - \alpha$ is equivalent to:*

$$\text{Prob}(t(x, \xi) = 1) \geq p_{N, \alpha}^*, \quad (4)$$

where $p_{N, \alpha}^* = g_N^{-1}(\alpha)$ is called the tree robustness threshold.

Proof. The following relationship holds for any forest of N base learners:

$$\text{Prob}(h_N(x, \xi) \geq 1/2) = \text{Prob}\left(\sum_{b=1}^N t_i(x, \xi) \geq N/2\right) = 1 - B(N/2; N, p(x)).$$

It follows from Lemma 1 that $1 - B(N/2; N, p(x)) \leq 1 - \alpha$ if and only if $g_N(p(x)) \geq \alpha$. \square

Theorem 1 provides a criterion to generate robust counterfactual explanations based on the probability of a single tree to predict the target class. We derive two properties from this relationship between forest robustness and tree robustness. The first one states how the tree robustness threshold varies as a function of the forest robustness threshold, and the second how the tree robustness threshold varies as a function of the forest size.

Proposition 1. *Let $N \in \mathbb{N}$, the tree robustness threshold $p_{N,\alpha}^*$ is monotonic increasing with the forest robustness threshold $(1 - \alpha)$.*

The proof follows directly from Lemma 1. This proposition confirms the intuitive property that a counterfactual explanation algorithm that is robust with a robustness level $(1 - \alpha)$ is also robust at robustness level lower than $(1 - \alpha)$. We now study how increasing the number of trees in the forest impacts robustness. We will need the following lemma.

Lemma 2. *Let $m \in \mathbb{N}$, the following relationships hold:*

- (a) $\forall \alpha \leq 1/2, p_{2m+3,\alpha}^* \leq p_{2m+1,\alpha}^*$,
- (b) $\forall \alpha \leq 1/2, p_{2(m+1),\alpha}^* \leq p_{2m,\alpha}^*$,
- (c) $\forall \alpha, p_{2m+1,\alpha}^* \leq p_{2m,\alpha}^*$.

The proof is based on studying the variations of $B(k; N, p)$ with fixed p and is given in Supplementary Material A.2.

Proposition 2. *If a counterfactual algorithm \mathcal{C} is robust to algorithmic uncertainty for forests with N trees and N is even, then it is also robust for any forest with more than N trees.*

The proof follows directly from Lemma 2. Proposition 2 generalizes the robustness of counterfactual explanations for a forest of size N . Remarkably, these results hold for any ensemble method that uses independently trained base learners, regardless of the re-sampling procedure (bootstrapping or sub-sampling) and the forest parameters (maximum depth, number of sub-sampled features, etc.). We illustrate the results of Proposition 1 and 2 in Figure 1, which shows how the tree robustness threshold $p_{N,\alpha}^*$ varies as a function of the forest robustness threshold $(1 - \alpha)$ and the forest size N .

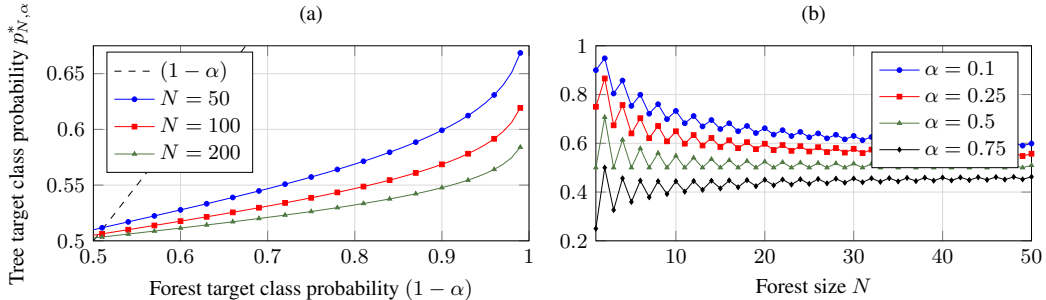


Figure 1: Sensitivity analysis of the tree robustness threshold $p_{N,\alpha}^*$.

3.2 Sample-average approximations of the tree robustness constraint

Theorem 1 provides a probabilistic constraint to generate robust counterfactuals. However, the resulting optimization model cannot be solved directly. It belongs to the class of chance-constrained models, which has been studied extensively in the stochastic optimization literature since the seminal work of Charnes and Cooper (1963). In general, the distribution of the class prediction $t(x, \xi)$ is unknown. However, it is possible to collect samples $\{t(x, \xi_i)\}_{i=1}^N$ by repeating the training procedure on the training set Z_n . In fact, given the initial forest F^0 , the tree samples $\{t^0(x, \xi_i^0)\}_{i=1}^N$

are already available, and are i.i.d. observations of $t(x, \xi)$. Thus, we can use the sample-average approximation (SAA), a well-known technique to solve chance-constrained problems (Pagnoncelli et al., 2009), to approximate the probabilistic constraint on tree robustness given in Equation (4).

Direct SAA. Given the tree samples $\{t^0(x, \xi_i^0)\}_{i=1}^N$, the SAA of the tree robustness constraint is:

$$h_N^0(x, \xi^0) \geq p_{N,\alpha}^*. \quad (5)$$

Since $p_{N,\alpha}^* \geq 1/2$ when $\alpha \leq 1/2$ (see Supplementary Material A.2), we can set the threshold τ in Problem (3) equal to $p_{N,\alpha}^*$ to obtain the SAA of the robust counterfactual explanation problem. Sample-average approximations of chance constraints have been shown to give good performance in numerous applications. However, with finite forest size N , the SAA may not always provide robust counterfactuals. Hence, we provide a more conservative formulation, that still uses only the initial forest and does not need to train any additional tree.

Robust SAA. The robust SAA is based on building a confidence interval around the tree robustness threshold $p_{N,\alpha}^*$ as if it were estimated from i.i.d. observations of a binomial distribution. When binomial samples are observed i.i.d., the sample mean is an unbiased minimum-variance estimator of the success rate p of the underlying Bernoulli distribution. Confidence intervals of the success rate of binomial distributions have been studied extensively. In particular, the Agresti-Coull (AC) confidence intervals (Agresti and Coull, 1998) have been shown to achieve good coverage of the true success rate in finite samples (Brown et al., 2001). Let \hat{p} be the empirical success rate measured for $\text{Bin}(N, p)$ where the true success rate p is unknown. The AC confidence interval is calculated as $C_{AC}^\beta = p_{AC} \pm z_{\beta/2} \sqrt{p_{AC}(1 - p_{AC})/N}$, where β is the error tolerance, $p_{AC} = (N\hat{p} + 2)/(N + 4)$ is the modified estimate of \hat{p} , and $z_{\beta/2} = \Phi^{-1}(1 - \beta/2)$ with Φ being the c.d.f. of the standard normal distribution.

We use the AC confidence interval to obtain a more conservative constraint than the direct SAA without increasing the forest size N . The robust SAA uses the target constraint:

$$h_N^0(x, \xi^0) \geq \rho_{N,\alpha,\beta}^*, \quad (6)$$

where $\rho_{N,\alpha,\beta}^* = p_{N,\alpha}^* + z_\beta \sqrt{\rho_{AC}(1 - \rho_{AC})/N}$ and $\rho_{AC} = (N \cdot p_{N,\alpha}^* + 2)/(N + 4)$. The confidence level $\beta \in [0, 1]$ is a hyperparameter that adjusts the conservativeness of the solution. As β increases, the robustness of the counterfactual increases and so does the distance to the initial observation. Thus, β depends on the data set and needs to be tuned according to the desired robustness level. The threshold τ in Problem (3) is thus set to $\rho_{N,\alpha,\beta}^*$. This threshold is always more conservative than $p_{N,\alpha}^*$ since $\beta = 0$ recovers the direct SAA.

3.3 Robustness guarantees for forests of stumps.

Although random forests are widely adopted in practice due to their high performance, they are much less understood from a theoretical standpoint. Consequently, simplifications of the original algorithm are commonly made to identify meaningful results (Biau and Scornet, 2016). Herein, we study random forests made of decision trees that use a single decision split, also called stumps. This simplified model has been studied for instance by Bühlmann and Yu (2002) to show how bagging reduces variance in random forests.

First, we show that the class prediction of tree stumps can be formulated as a convex constraint for any realization of the uncertain training procedure. Let $\mathcal{X} \subseteq [0, 1]^d$ and $t(x, \xi)$ be a decision stump. The tree robustness constraint can be expressed equivalently as a convex constraint as:

$$\text{Prob}(t(x, \xi) = 1) = \text{Prob}(A(\xi)^\top x - b(\xi) \leq 0), \quad (7)$$

where $A(\xi) \in \{-1, 0, 1\}^d$ and $b(\xi) \in [-1, 1]$. The vector $A(\xi)$ is such that $a_j(\xi) = 0$ if the stump does not split on feature j , $a_j(\xi) = 1$ if it splits on feature j and the left leaf node has class 1 and $a_j(\xi) = -1$ if it splits on feature j and the right leaf node has class 1. The split threshold $b(\xi)$ is positive if the left leaf node has class 1 and negative otherwise. Thus, the function on the left-hand side of the probabilistic Constraint (7) is convex in x . This reformulation allows us to leverage existing results on the approximation of chance constraints to obtain asymptotic and finite-samples robustness guarantees for random forests of stumps.

Proposition 3 (Asymptotic consistency). *As the forest size N increases, the solution of the direct SAA model converges almost surely to the minimum-cost robust counterfactual explanation.*

Having shown that the tree class prediction constraint is convex, the proof follows directly from Shapiro et al. (2014, Chapter 5). Proposition 3 ensures that the robustness of counterfactual explanations obtained by solving Problem (3) with the direct SAA method increases as the forest size increases. However, it may not be possible to train additional trees when determining counterfactual explanations, for instance if only the initial forest F^0 is available.

In this case, we are interested in finite-sample robustness guarantees for solving Problem (3) with a fixed forest size. Finite-samples bounds on the quality of the SAA solution have been studied by Luedtke and Ahmed (2008), but they require stringent assumptions on the feature space \mathcal{X} that do not hold if the feature vector contains both continuous and discrete features. A second approximation technique, called the convex approximation, can be used in this setting. The convex approximation of the tree robustness constraint results in the following set of constraints:

$$t^0(x, \xi_i^0) = 1, \forall i \in \{1, \dots, N\}.$$

Thus, solving Problem (3) with $\tau = 1$ is the convex approximation of the robust counterfactual explanation problem. Finite-sample bounds can be derived on the probability of finding a robust solution by solving the convex approximated model. Campi and Garatti (2008) provide a key result when the feasible set \mathcal{X} is convex and De Loera et al. (2018) generalize it to decision variables that take both continuous and discrete values. We can apply the latter result to forests of stumps to obtain the following bound.

Proposition 4 (Finite-sample guarantees). *Given a forest of size N and a feature vector x with k continuous features and $d - k$ discrete features, if a solution to the convex approximated problem exists, the probability that it is a robust counterfactual explanation is at least $(1 - \delta)$ with $\delta = \exp \left[(2^{d-k}(k+1) - 1) (\log(1/\alpha) + \alpha) - (\alpha/2)N \right]$.*

The proof follows directly from De Loera et al. (2018) since the tree robustness constraint is convex in x . Note that this probability guarantee decreases exponentially as the number of trees increases.

4 Numerical study

We conduct extensive experiments to (i) evaluate the robustness of our proposed approaches, (ii) understand why counterfactual explanations have varying robustness on different data sets, and (iii) demonstrate that our method provides the best trade-off between counterfactual robustness and distance among existing counterfactual generation methods.

The simulations are implemented in Python 3.9 using scikit-learn v.1.0.2 to train the random forests. We model Problem (1) as a MILP using the OCEAN package from Parmentier and Vidal (2021). Gurobi 9.5 is used to solve the resulting optimization problem. All experiments are run on an Intel(R) Core(TM) i7-11800H processor at 2.30Ghz using 16GB of RAM. The data sets have been pre-processed following Parmentier and Vidal (2021) to ignore missing values and to take into account feature actionability. A summary of the data sets considered is provided in Supplementary Material B.1. The code to reproduce all results and figures in this paper is made publicly available at <https://github.com/alexforel/RobustCF4RF> under an MIT license.

4.1 Simulation setting

We build random forests of $B = 100$ decision trees with a maximum depth of 4. In the training phase, each tree uses a bootstrap re-sample of the training set and \sqrt{p} randomly selected features to find the best split at each node. In each simulation, $N_{\text{IN}} = 5$ samples are selected randomly from the data set to serve as new observations for which to derive counterfactuals. A first forest F^0 is trained on the remaining $(n - N_{\text{IN}})$ points. Counterfactuals are generated by solving Problem (3) with the relevant classification threshold. A second forest F is trained on the same data to assess if the counterfactual explanations are valid. We repeat this procedure $N_{\text{SIM}} = 40$ times.

We implement the direct SAA and robust SAA methods with $\beta \in \{0.05, 0.1\}$. The key performance indicators are the distance between the initial observation and the counterfactual and their validity,

measured as the percentage of counterfactuals that are valid to the test classifier. The distance measure is set to a feature-weighted l_1 norm. To calibrate the cost of feature changes between continuous and non-continuous features, we reduce the weight of changes on non-continuous features by a factor 1/4. We vary the robustness target level by letting $\alpha \in \{0.5, 0.4, 0.3, 0.2, 0.15, 0.1, 0.05, 0.01\}$.

We implement three benchmarks to assess the value of our robust methods: (1) the naive approach that uses the sample-average constraint $h_N(x) \geq 1/2$, (2) a plausibility-based benchmark that uses isolation forests (Parmentier and Vidal, 2021; Liu et al., 2008), and (3) a plausibility-based benchmark that uses the local outlier factor as Kanamori et al. (2020). The contamination parameter of the isolation forest method is varied as $c \in \{0.05, 0.1, 0.2, 0.3, 0.4, 0.5\}$. Similarly, the weight of the local outlier factor penalty term is varied as $\lambda \in \{1e^{-3}, 1e^{-2}, 1e^{-1}, 1, 1e^1, 1e^2\}$ following Kanamori et al. (2020). Details on the implementation and computation times are provided in Supplementary Material B.2.

4.2 Achieving robust counterfactual explanations

Example. We illustrate the generated counterfactual explanations with varying robustness targets for the German Credit data set in Figure 2. An initial observation and its feature values are shown as a heatmap. We show the changes to the initial feature values as the target robustness level $(1 - \alpha)$ increases. The change can be positive or negative. Figure 2 illustrates how the number and magnitude of feature changes vary as $(1 - \alpha)$ increases. Interestingly, the trajectory is not linear as the robustness target increases. Instead, a few key features are perturbed at each robustness target level. Additional examples are available in Supplementary Material B.3.

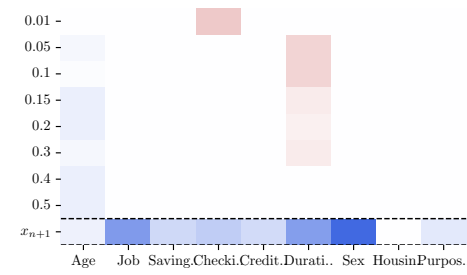


Figure 2: Initial observation and counterfactual explanations for increasing $(1 - \alpha)$.

Algorithmic robustness. The validity of the counterfactual explanations generated by the Direct- and Robust-SAA methods is shown in Figure 3 for varying robustness target levels. For each robustness target level, a binomial hypothesis test is performed to measure whether the achieved validity equals the robustness target level. The confidence interval at the 0.05 level is shown as a colored area. Figure 3 shows that the Direct-SAA method provides robust counterfactual explanations on all but one data sets. When the robustness target $(1 - \alpha)$ is small, counterfactual explanations with high robustness can be found in two data sets: COMPAS and Phishing. Conversely, the data set Spambase with $d = 57$ continuous features proves the most difficult. It is only on this instance that the Robust-SAA method is required. The Robust-SAA method yields robust counterfactuals for moderate and high robustness levels with $\beta = 0.1$ and $\beta = 0.05$, respectively.

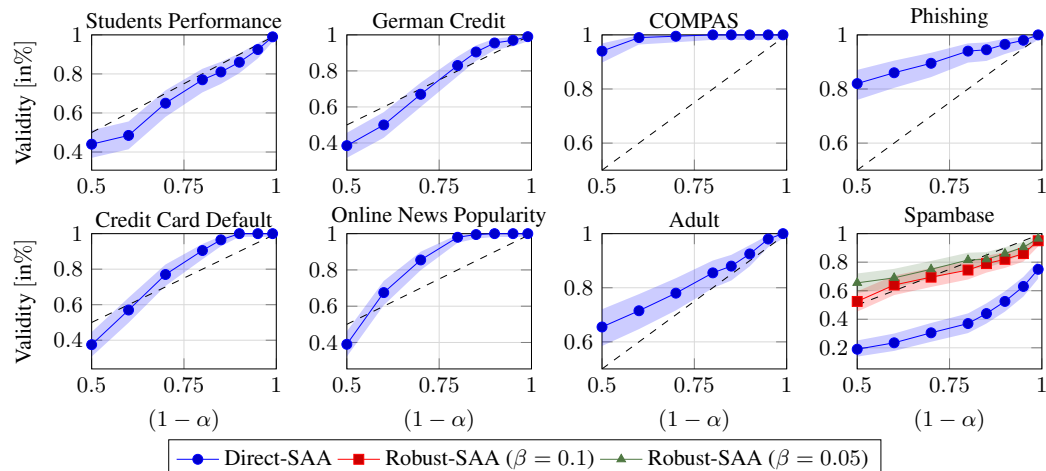


Figure 3: Validity of robust counterfactuals as a function of the robustness target $(1 - \alpha)$.

To explain the varying robustness achieved on the different data sets, we analyze two aspects: (i) the average number of features changed in counterfactual explanations, and (ii) the link between the changed features and their predictive importance. The analysis of feature importance is provided in Supplementary Material B.4. It shows that feature changes in counterfactual explanations follow largely their predictive importance: highly predictive features have large changes, whereas unimportant features are mostly unchanged.

Figure 4 shows the average number of changed features as a function of the robustness target level. Overall, data sets that have a few key features with high importance exhibit sparse and robust counterfactual explanations. This is especially true if the features are discrete or categorical. This sparsity leads to robust counterfactual explanations, even when the robustness target level is low. On the contrary, data sets that have many important features have low inherent robustness.

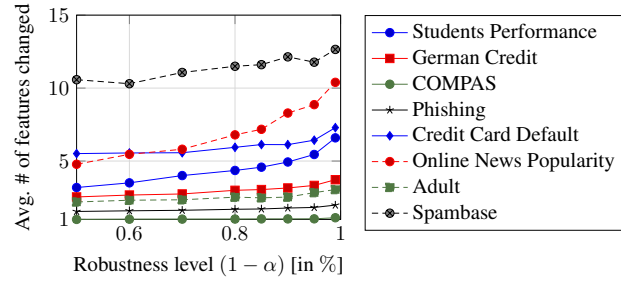


Figure 4: Features changed for varying robustness $(1 - \alpha)$.

Trade-off between counterfactual distance and robustness. The counterfactual distance and validity of the proposed methods and benchmarks are shown in Figure 5. On most data sets, our methods yield robust counterfactuals with only a slight increase in distance. A sensitivity analysis of the distance of robust counterfactuals is provided in Supplementary Material B.5. Figure 5 shows that our methods strictly dominate the naive and plausibility-based benchmarks and generate the Pareto front of dominant solutions. This means that plausibility and robustness are independent in practice. Even with high contamination parameters, isolation forests (IForest) do not provide robust explanations although they substantially increase counterfactual distance. Increasing the penalty factor of the local outlier factor (1-LOF) method slightly increases robustness but leads to significantly more distant counterfactual explanations than the ones generated by our robust methods.

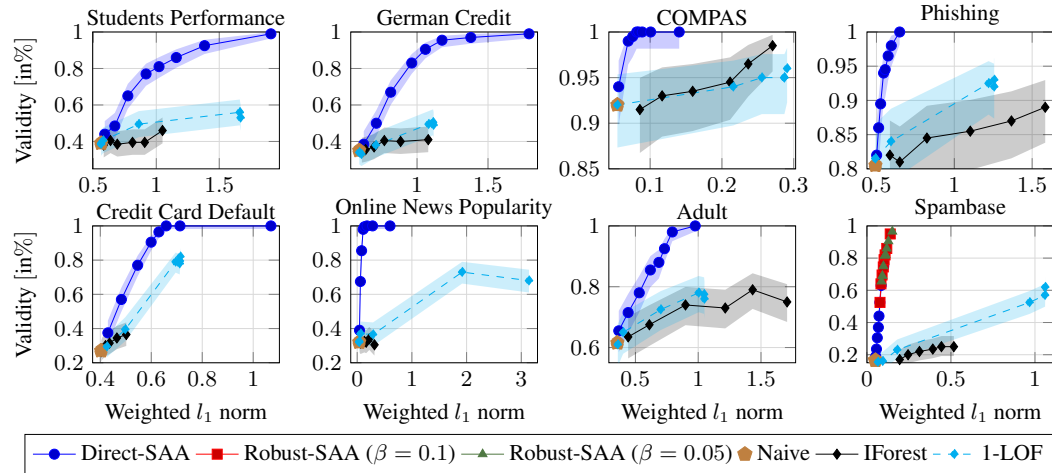


Figure 5: Trade-off between counterfactual distance and robustness.

5 Conclusions and broader impact

This work sheds light on a critical, yet overlooked, aspect of interpretability in machine learning: the lack of robustness of existing counterfactual explanation methods. We contribute to building more transparent classifiers by providing an effective and easy-to-implement approach to improve robustness. Our method is supported by a probabilistic analysis of classification ensembles and its value has been demonstrated on real-world data. To help practitioners identify situations in

which robust counterfactual explanations are essential, we derive valuable insights regarding the link between the robustness of counterfactual explanations and the characteristics of the data sets.

Future work could investigate how to generalize the proposed methodology when the base learners of a classification ensemble are not trained independently, such as forests of boosted trees. Another interesting direction is to study the robustness of counterfactuals to sampling uncertainty: when the test model is re-trained with additional samples obtained from the same distribution.

References

M. Abramowitz, I. A. Stegun, and R. H. Romer. *Handbook of mathematical functions with formulas, graphs, and mathematical tables*. American Association of Physics Teachers, 1988.

A. Agresti and B. A. Coull. Approximate is better than “exact” for interval estimation of binomial proportions. *The American Statistician*, 52(2):119–126, 1998.

A. Artelt and B. Hammer. Convex density constraints for computing plausible counterfactual explanations. In *International Conference on Artificial Neural Networks*, pages 353–365. Springer, 2020.

G. Biau and E. Scornet. A random forest guided tour. *Test*, 25(2):197–227, 2016.

O. Bousquet and A. Elisseeff. Stability and generalization. *Journal of Machine Learning Research*, 2:499–526, 2002.

L. Breiman. Random forests. *Machine Learning*, 45(1):5–32, 2001.

L. Breiman, J. H. Friedman, R. A. Olshen, and C. J. Stone. *Classification and regression trees*. Routledge, 1984.

L. D. Brown, T. T. Cai, and A. DasGupta. Interval estimation for a binomial proportion. *Statistical Science*, 16(2):101–133, 2001.

P. Bühlmann and B. Yu. Analyzing bagging. *The Annals of Statistics*, 30(4):927–961, 2002.

N. Bui, D. Nguyen, and V. A. Nguyen. Counterfactual plans under distributional ambiguity. In *International Conference on Learning Representations*, 2022.

M. C. Campi and S. Garatti. The exact feasibility of randomized solutions of uncertain convex programs. *SIAM Journal on Optimization*, 19(3):1211–1230, 2008.

A. Charnes and W. W. Cooper. Deterministic equivalents for optimizing and satisficing under chance constraints. *Operations Research*, 11(1):18–39, 1963.

Z. Cui, W. Chen, Y. He, and Y. Chen. Optimal action extraction for random forests and boosted trees. In *Proceedings of the 21th ACM SIGKDD International Conference on Knowledge Discovery and Data Mining*, pages 179–188, 2015.

J. A. De Loera, R. N. La Haye, D. Oliveros, and E. Roldán-Pensado. Chance-constrained convex mixed-integer optimization and beyond: Two sampling algorithms within S -optimization. *Journal of Convex Analysis*, 25(1):201–218, 2018.

T. Hastie, R. Tibshirani, and J. H. Friedman. *The elements of statistical learning: data mining, inference, and prediction*, volume 2. Springer, 2009.

K. Kanamori, T. Takagi, K. Kobayashi, and H. Arimura. DACE: Distribution-aware counterfactual explanation by mixed-integer linear optimization. In *International Joint Conference on Artificial Intelligence*, pages 2855–2862, 2020.

T. Laugel, M.-J. Lesot, C. Marsala, X. Renard, and M. Detyniecki. The dangers of post-hoc interpretability: Unjustified counterfactual explanations. In *International Joint Conference on Artificial Intelligence*, pages 2801–2807, 2019.

F. T. Liu, K. M. Ting, and Z.-H. Zhou. Isolation forest. In *Eighth IEEE International Conference on Data Mining*, pages 413–422. IEEE, 2008.

M. E. Lopes. Estimating the algorithmic variance of randomized ensembles via the bootstrap. *The Annals of Statistics*, 47(2):1088–1112, 2019.

J. Luedtke and S. Ahmed. A sample approximation approach for optimization with probabilistic constraints. *SIAM Journal on Optimization*, 19(2):674–699, 2008.

B. K. Pagoncelli, S. Ahmed, and A. Shapiro. Sample average approximation method for chance constrained programming: theory and applications. *Journal of Optimization Theory and Applications*, 142(2):399–416, 2009.

A. Parmentier and T. Vidal. Optimal counterfactual explanations in tree ensembles. In *International Conference on Machine Learning*, pages 8422–8431. PMLR, 2021.

M. Pawelczyk, K. Broelemann, and G. Kasneci. On counterfactual explanations under predictive multiplicity. In *Conference on Uncertainty in Artificial Intelligence*, pages 809–818. PMLR, 2020.

P. Probst and A.-L. Boulesteix. To tune or not to tune the number of trees in random forest. *Journal of Machine Learning Research*, 18(1):6673–6690, 2017.

K. Rawal, E. Kamar, and H. Lakkaraju. Can i still trust you?: Understanding the impact of distribution shifts on algorithmic recourses. *arXiv preprint arXiv:2012.11788*, 2020.

A. Shapiro, D. Dentcheva, and A. Ruszczynski. *Lectures on stochastic programming: modeling and theory*. SIAM, 2014.

S. Upadhyay, S. Joshi, and H. Lakkaraju. Towards robust and reliable algorithmic recourse. In *Advances in Neural Information Processing Systems*, 2021.

B. Ustun, A. Spangher, and Y. Liu. Actionable recourse in linear classification. In *Conference on Fairness, Accountability, and Transparency*, pages 10–19, 2019.

S. Wachter, B. Mittelstadt, and C. Russell. Counterfactual explanations without opening the black box: Automated decisions and the GDPR. *Harvard Journal of Law & Technology*, 31:841, 2017.

A Supplementary material: Proofs

A.1 Proof of Lemma 1

The c.d.f. of the binomial distribution can be expressed in terms of the regularized incomplete beta function $I_x(a, b)$ as $g_N(p) = I_{1-p}(N/2, N/2 + 1)$ (Abramowitz et al., 1988, Section 26.5). Since $I_x(a, b)$ is the c.d.f. of the beta distribution, $I_x(a, b)$ is increasing in x and is invertible, so that $g_N(p)$ is decreasing in p and is also invertible.

A.2 Proof of Lemma 2

Lemma 2 is obtained by studying the sequence $f_N : N \mapsto B(N/2; N, p)$ with fixed p . Interestingly, this sequence is not monotonic in N and we need to analyze separately the cases of odd and even integers. We will need the following lemma.

Lemma 3. *Given $N \in \mathbb{N}$, $\alpha \leq 1/2 \Rightarrow p_{N,\alpha}^* \geq 1/2$.*

Proof. Given $\alpha \in [0, 1/2]$, we know from Lemma 1 that $p_{N,\alpha}^* \geq p_{N,1/2}^*$. We have

$$p_{N,1/2}^* \geq 1/2 \iff g_N(p_{N,1/2}^*) \leq g_N(1/2) \iff 1/2 \leq B(N/2; N, 1/2),$$

since g_N is decreasing. Notice that the latest condition is true for all N since $B(N/2; N, 1/2) = 1/2$ when N is odd and $B(N/2; N, 1/2) < 1/2$ when N is even. \square

Proof of Lemma 2(a). We focus first on odd integers. Define $S_N \sim \text{Bin}(N, p)$ and let $m \in \mathbb{N}$. The c.d.f. of the binomial distribution is:

$$\begin{aligned} B(m+1; 2m+3, p) &= \text{Prob}(S_{2m+3} \leq m+1) \\ &= \text{Prob}(S_{2m+3} \leq m+1 \mid S_{2m+1} \leq m-1) \text{Prob}(S_{2m+1} \leq m-1) \\ &\quad + \text{Prob}(S_{2m+3} \leq m+1 \mid S_{2m+1} = m) \text{Prob}(S_{2m+1} = m) \\ &\quad + \text{Prob}(S_{2m+3} \leq m+1 \mid S_{2m+1} = m+1) \text{Prob}(S_{2m+1} = m+1) \\ &= \text{Prob}(S_{2m+1} \leq m-1) + (1-p^2) \text{Prob}(S_{2m+1} = m) \\ &\quad + (1-p)^2 \text{Prob}(S_{2m+1} = m+1). \end{aligned}$$

Notice that

$$\text{Prob}(S_{2m+1} \leq m-1) = \text{Prob}(S_{2m+1} \leq m) - \text{Prob}(S_{2m+1} = m) \quad (8)$$

and, because of the symmetry of the binomial coefficients,

$$(1-p)^2 \text{Prob}(S_{2m+1} = m+1) = p(1-p) \text{Prob}(S_{2m+1} = m). \quad (9)$$

By combining Equations (8) and (9), the difference between f_{2m+3} and f_{2m+1} can be expressed as

$$B(m+1; 2m+3, p) - B(m; 2m+1, p) = p(1-2p) \text{Prob}(S_{2m+1} = m),$$

which is negative if and only if $p \geq 1/2$.

To finish the proof, let $\alpha \leq 1/2$ and notice that, given the definition of $p_{N,\alpha}^*$, we have

$$\alpha = B(m+1; 2m+3, p_{2m+3,\alpha}^*) = B(m; 2m+1, p_{2m+1,\alpha}^*). \quad (10)$$

Since $\alpha \leq 1/2$, we know from Lemma 3 that $p_{2m+1,\alpha}^* \geq 1/2$ and therefore:

$$B(m; 2m+1, p_{2m+1,\alpha}^*) \geq B(m+1; 2m+3, p_{2m+1,\alpha}^*). \quad (11)$$

By combining Equations (10) and (11), we obtain

$$B(m+1; 2m+3, p_{2m+3,\alpha}^*) \geq B(m+1; 2m+3, p_{2m+1,\alpha}^*),$$

which is only true when $p_{2m+1,\alpha}^* \geq p_{2m+3,\alpha}^*$ since g_N is decreasing according to Lemma 1.

Proof of Lemma 2(b). We focus now on even integers. We can similarly determine the difference between $f_{2(m+1)}$ and f_{2m} as

$$B(m+1; 2(m+1), p) - B(m; 2m, p) = (1-p)^2 \text{Prob}(S_{2m} = m+1) - p^2 \text{Prob}(S_{2m} = m),$$

so that

$$\begin{aligned} f_{2(m+1)} - f_{2m} &= p^{m+1}(1-p)^m \left[(1-p) \binom{2m}{m+1} - p \binom{2m}{m} \right] \\ &= p^{m+1}(1-p)^m (2m)! \left[\frac{1-p}{(m+1)!(m-1)!} - \frac{p}{(m!)^2} \right] \\ &= p^{m+1}(1-p)^m (2m)! \frac{\text{Num}(p)}{(m+1)!(m-1)!(m!)^2} \end{aligned}$$

where $\text{Num}(p) = m \cdot (m-1)! [(1-p)m - p(m+1)]$. Thus, f_{2m} is greater than $f_{2(m+1)}$ if and only if $\text{Num}(p) \leq 0$ that is

$$p \geq \frac{m}{2m+1}.$$

Since $m/(2m+1) < 1/2$ for all $m > 0$, $B(m+1; 2(m+1), p) \leq B(m; 2m, p)$ when $p \geq 1/2$.

To finish the proof, let $\alpha \leq 1/2$ be such that:

$$\alpha = B(m+1; 2(m+1), p_{2(m+1), \alpha}^*) = B(m; 2m, p_{2m, \alpha}^*). \quad (12)$$

Since $B(m+1; 2(m+1), p_{2(m+1), \alpha}^*) \leq B(m; 2m, p_{2(m+1), \alpha}^*)$, we have from (12) that:

$$B(m; 2m, p_{2m, \alpha}^*) \leq B(m; 2m, p_{2(m+1), \alpha}^*),$$

which is true when $p_{2m, \alpha}^* \geq p_{2(m+1), \alpha}^*$ since g_N is decreasing according to Lemma 1.

Proof of Lemma 2(c). Let $m \in \mathbb{N}$, we have

$$\begin{aligned} B(m; 2m+1, p) &= \text{Prob}(S_{2m+1} \leq m) \\ &= \text{Prob}(S_{2m+1} \leq m \mid S_{2m} \leq m-1) \text{Prob}(S_{2m} \leq m-1) \\ &\quad + \text{Prob}(S_{2m+1} \leq m \mid S_{2m} = m) \text{Prob}(S_{2m} = m) \\ &= \text{Prob}(S_{2m} \leq m-1) + (1-p) \text{Prob}(S_{2m} = m). \end{aligned}$$

Because

$$\text{Prob}(S_{2m} \leq m) = \text{Prob}(S_{2m} \leq m-1) + \text{Prob}(S_{2m} = m),$$

the difference

$$f_{2m+1} - f_{2m} = -p \text{Prob}(S_{2m} = m)$$

is negative for all $p \in [0, 1]$. Hence, let α be such that:

$$\alpha = B(m; 2m, p_{2m, \alpha}^*) = B(m; 2m+1, p_{2m+1, \alpha}^*). \quad (13)$$

Since $B(m; 2m+1, p_{2m, \alpha}^*) \leq B(m; 2m, p_{2m, \alpha}^*)$, we have from (13) that:

$$B(m; 2m+1, p_{2m, \alpha}^*) \leq B(m; 2m+1, p_{2m+1, \alpha}^*),$$

which is true when $p_{2m, \alpha}^* \geq p_{2m+1, \alpha}^*$ since g_N is decreasing according to Lemma 1.

B Supplementary material: Numerical study

B.1 Summary of data sets

A summary of the data sets is given in Table 1, where n is the size of the training set, d the number of features, and (d_B, d_C, d_D, d_N) the number of binary, categorical, discrete numerical, and continuous numerical features, respectively.

B.2 Implementation details

In this section, we provide additional details on the implementation of our methods as well as the formulation of the plausibility-based benchmarks.

Table 1: Summary of the data sets.

Data set	n	d	d_B	d_C	d_D	d_N	Source
Adult	45222	11	2	4	3	2	UCI
Credit Card Default	29623	14	3	0	11	0	UCI
COMPAS	5278	5	2	0	3	0	ProPublica
German Credit	1000	9	0	3	5	1	UCI
Online News	39644	47	2	2	6	37	UCI
Data Phishing	11055	30	8	0	22	0	UCI
Spambase	4601	57	0	0	0	57	UCI
Students Performance	395	30	13	4	13	0	UCI

SAA-based methods. The SAA-based methods such as Direct-SAA, Robust-SAA and the naive benchmark are implemented directly using the formulation of Parmentier and Vidal (2021) and its openly available implementation. The constraint on the target classification score in (3b) is adapted for each method: $\tau = 1/2$ for the naive benchmark, $\tau = p_{N,\alpha}^*$ for the Direct-SAA, and $\tau = \rho_{N,\alpha,\beta}^*$ for the Robust-SAA.

When the robustness target is high, the resulting optimization problem might be infeasible, for instance, due to the actionability constraints. Thus, we relax Constraint (3b) defining the target classification score, and add a penalty cost $z_{pen} = 5000 \cdot d$ where d is the number of features. The objective of Problem (3) is then

$$f(x, x_{n+1}) + z_{pen} \cdot \nu,$$

where ν is the relaxation term, and the relaxed constraint is:

$$h_N^0(x, \xi^0) \geq \tau - \nu.$$

Isolation forests. Isolation forests have been used by Parmentier and Vidal (2021) to ensure that the counterfactual explanation is not an outlier of the target sample distribution. Isolation forests measure the anomaly of an observation by comparing the path length of the isolation forest to the average path length of a binary search tree. This plausibility-based benchmark is implemented as follows. First, an isolation forest of size $N_{IF} = 50$ trees is trained on the samples of the training set with the target class. The isolation forest is trained using scikit-learn. The contamination parameter is varied as explained in Section 4 and the other parameters are kept at their default values. The contamination parameter impacts the conservativeness of the model: the higher the contamination parameter, the higher the percentage of samples of the distribution that are classified as outliers. Then, the counterfactual explanation model is solved with additional constraints to state that the counterfactual is not classified as an outlier by the isolation forest.

We modify the formulation of Parmentier and Vidal (2021) to allow varying contamination parameters. Let \mathcal{T}_{IF} be the sets of isolation trees and \mathcal{V}_t^L the set of leaf nodes of tree t . Denote by δ_v the depth of leaf node v and by $c(n)$ the average path length of a binary search tree using n samples. Following the implementation of Parmentier and Vidal (2021), the decision variable indicates $y_{v,t}$ is equal to 1 if the counterfactual explanation ends in leaf node v of tree t . The plausibility constraints are implemented as:

$$I_t = \sum_{v \in \mathcal{V}_t^L} (\delta_v + c(n_{v,t})) y_{v,t}, \quad \forall t \in \mathcal{T}_{IF} \quad (14)$$

$$A = \frac{1}{N_{IF}} \sum_{t \in \mathcal{T}_{IF}} \frac{I_t}{c(n)}, \quad (15)$$

$$A \leq \log(-I_{OFF}) / \log(2) + \nu, \quad (16)$$

$$I_t, A, \nu \geq 0. \quad (17)$$

Constraint (14) measures the depth of the isolation trees, where $n_{v,t}$ is the number of samples in leaf node v of tree t . Constraint (15) measures the anomaly of the counterfactual and Constraint (16) restricts the anomaly of the counterfactual to be below the classification threshold of the trained isolation forest. The parameter I_{OFF} is the forest offset that depends on the contamination parameter, following the scikit-learn implementation. As for the SAA-based methods, ν is a decision variable that relaxes the problem in case of infeasibility and is penalized with a large cost in the objective.

Local outlier factor. The local outlier factor (LOF) is an outlier detection method used by Kanamori et al. (2020) to ensure the plausibility of counterfactual explanations. It is based on measuring the proximity of an observation to a distribution by comparing the distance of samples to their nearest neighbors. Kanamori et al. (2020) use the 1-LOF, a simpler implementation of the general k-LOF method in which only the nearest neighbor is considered.

The 1-LOF is implemented as a penalty term added to the objective function of Problem (1) as:

$$f(x, x_{n+1}) + \sum_{i=1}^n l^{(i)} \cdot \rho_i,$$

where $l^{(i)}$ is the local reachability density of the training sample x_i and ρ_i is a decision variable that measures the reachability distance of x . The local reachability density measures how close a sample is to its nearest neighbors. In the 1-LOF case, the local reachability density is expressed as $l^{(i)} = lrd(x_i) = \Delta(1NN(x_i))^{-1}$, where $1NN(x_n)$ is the nearest neighbor of x_n and $\Delta(x)$ is the distance between x and its nearest neighbor. The reachability distance of x and x_i is the maximum between the distance between x and x_i and the distance between x_i and its nearest neighbor. Finding the reachability distance of x is implemented through the following constraints:

$$\begin{aligned} \sum_{i=1}^n \nu_i &= 1, \\ f(x_{i_1}, x_{i_2}) &\leq (1 - \nu_{i_1}) \cdot d, & \forall i_1, i_2 \in \{1, \dots, n\}, \\ \rho_i &\geq \Delta(x_i) \cdot \nu_i, & \forall i \in \{1, \dots, n\}, \\ \rho_i &\geq f(x, x_i) - (1 - \nu_i) \cdot d, & \forall i \in \{1, \dots, n\}, \\ \nu_i &\in \{0, 1\}, \rho_i \geq 0 & \forall i \in \{1, \dots, n\}. \end{aligned}$$

The binary variable ν_i tracks the nearest neighbor of x in the training set. This method does not scale to large problem instances. In particular, the number of constraints grows quadratically in the number of samples in the training set. Thus, we simplify the formulation by restricting the number of training samples considered. We implement the above constraints only for the $N_r = 10$ nearest neighbors of the initial observation x_{n+1} . This allows us to repeatedly obtain counterfactual explanations using the 1-LOF plausibility constraints on all data sets and for all penalty factors λ . Interestingly, the "Online News Popularity" data set is still challenging to solve to optimality for $\lambda \geq 0.1$. In this case, we further reduce the relative MIP optimality gap parameter of the solver to 10%. Thus, we can apply the 1-LOF method on larger, more diverse data sets than Kanamori et al. (2020), who impose a time limit of 600 seconds to solve the optimization model.

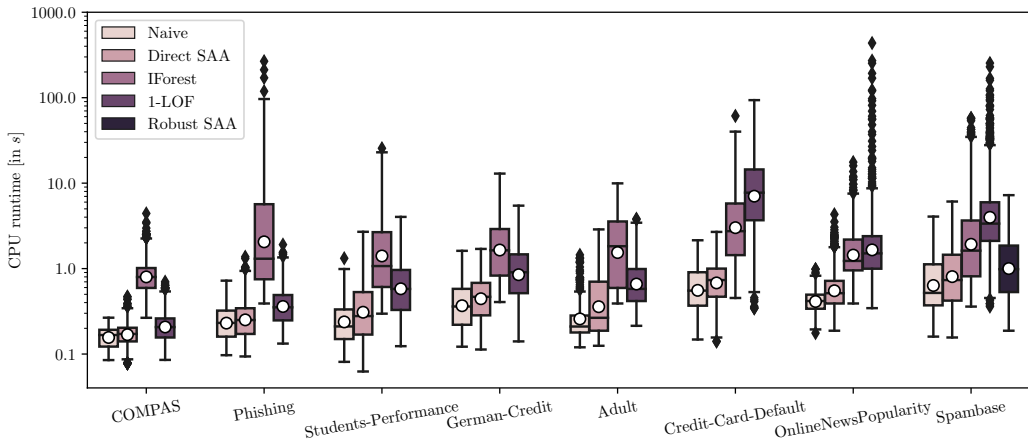


Figure 6: Boxplot of computation times over the different data sets.

Computation times. We show the computation times to solve the optimization models of all the implemented methods in Figure 6. For each data set and for each method, we show the boxplot of the runtimes for all parameters (e.g. for all values of α in the Direct-SAA case). The figure shows

that the Direct-SAA method has only little increase in computation times compared to the naive benchmark. Conversely, the plausibility-based benchmarks have large increase in computational times, especially for the large data sets.

B.3 Examples of counterfactual explanations for varying robustness levels

We provide additional examples of counterfactual explanations for increasing robustness levels. Figures 7 and 8 illustrate the counterfactual explanations obtained on the Adult and Credit Card Default data sets, respectively. Interestingly, the counterfactual explanations on the first data set are very sparse and involve only a few features. In contrast, the counterfactual explanations obtained on the second data set involve more diverse feature perturbations. It is also interesting to observe that the counterfactual explanations are sometimes not modified as the robustness level increases. This threshold effect is due to the discrete values of the modified features.

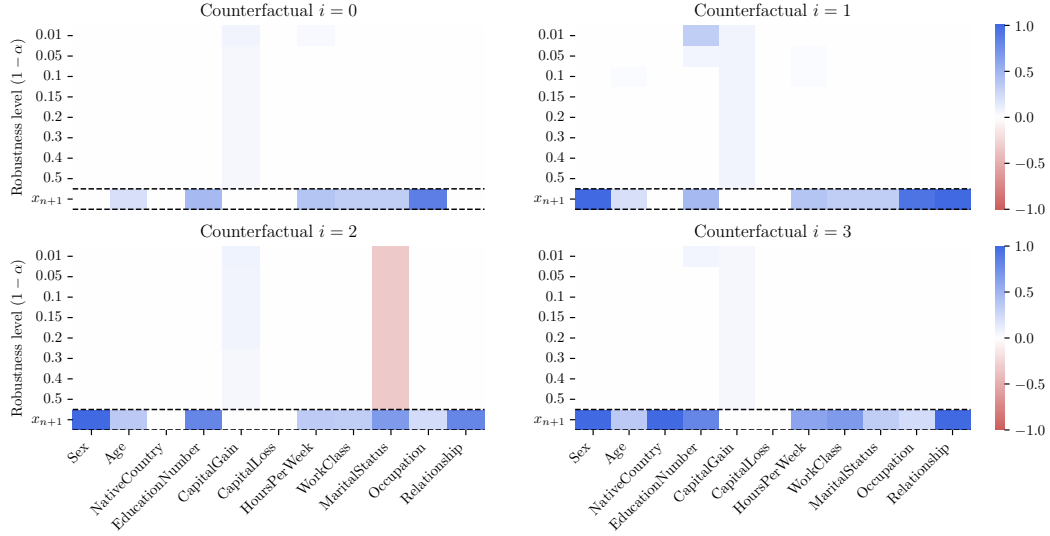


Figure 7: Adult: initial observation and counterfactual changes to reach the target class for increasing robustness level $(1 - \alpha)$.

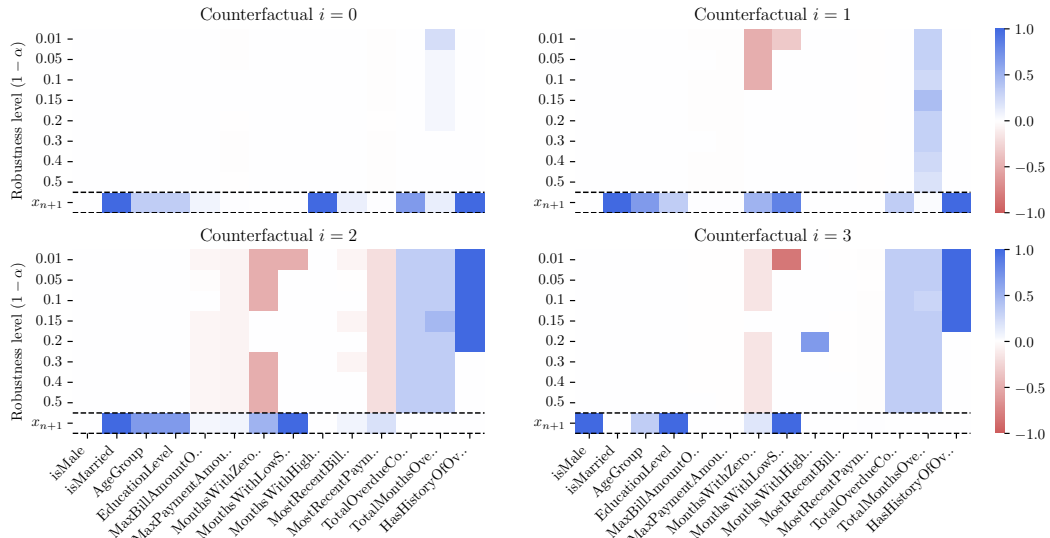


Figure 8: Credit Card Default: initial observation and counterfactual changes to reach the target class for increasing robustness level $(1 - \alpha)$.

B.4 Feature importance, sparsity, and robustness

We investigate the link between the feature changes from the counterfactual explanations and the predictive importance of the features. We measure the feature importance by using the permutation method of Breiman (2001). We also measure the average absolute changes to the features of counterfactual explanations given by the Direct-SAA method with robustness target $(1 - \alpha) = 0.5$. We show the feature importance and average feature changes in Figures 9 and 10 for two data sets with high robustness and two data sets with low robustness, respectively. The feature importance and changes are normalized to better compare the two measures. Remarkably, feature importance and the average feature changes are very similar on all data sets. Some of the main differences between feature importance and feature changes can be explained by the actionability constraints. For instance, the "AgeGroup" feature can only increase in the COMPAS data set. The data sets shown in Figure 9 have especially sparse important features. It is also for these two data sets that the robustness of naive explanations is the highest. This suggests that having a few features with high importance favors obtaining robust naive counterfactual explanations. Conversely, a data set with many important features is a good indicator that robustness should be explicitly considered when generating counterfactual explanations.

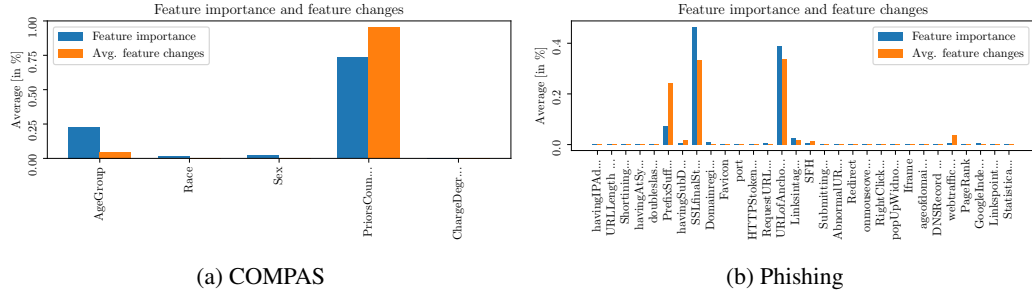


Figure 9: Feature importance and feature changes for two data sets with high robustness.

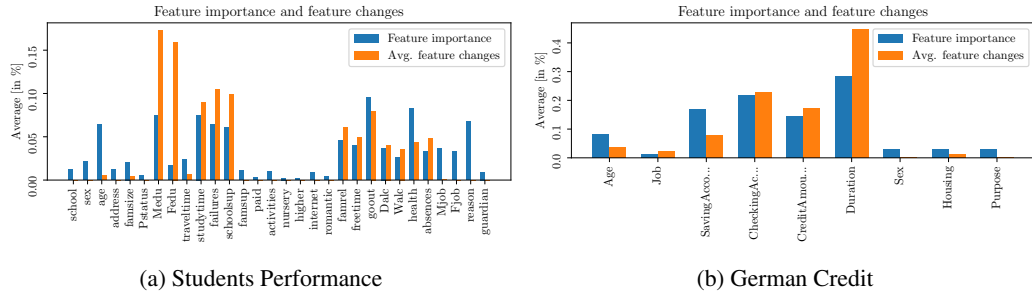


Figure 10: Feature importance and feature changes for two data sets with low robustness.

B.5 Sensitivity analysis: robustness target and counterfactual distance

The impact of the robustness target on the distance of counterfactual explanations is shown in Figure 11. One standard deviation of the distance is also shown in a colored area. The high variance of the counterfactual distance is due to the fact that the initial observations are picked randomly from the training set. Figure 11 shows that robust explanations can be obtained with only a small distance increase for moderate robustness target levels, but the highest robustness levels are only attained with an exponential increase in counterfactual distance.

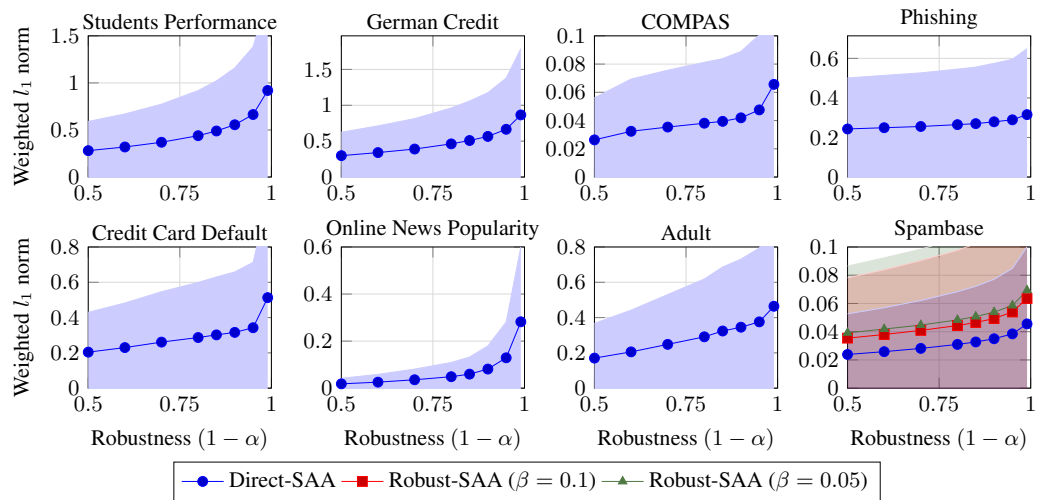


Figure 11: Distance of robust counterfactuals for varying robustness target $(1 - \alpha)$.